

# Scalable quantum computing with atomic ensembles

Sean D. Barrett,<sup>1,\*</sup> Peter P. Rohde,<sup>2,†</sup> and Thomas M. Stace<sup>3,‡</sup>

<sup>1</sup>*Blackett Laboratory, Imperial College London, Prince Consort Road, London SW7 2BZ, United Kingdom*

<sup>2</sup>*Department of Materials, University of Oxford, Parks Road, Oxford, OX1 3PH, UK*

<sup>3</sup>*Department of Physics, University of Queensland, Brisbane, QLD 4072, Australia*

(Dated: October 31, 2018)

Atomic ensembles, comprising clouds of atoms addressed by laser fields, provide an attractive system for both the storage of quantum information, and the coherent conversion of quantum information between atomic and optical degrees of freedom. In a landmark paper, Duan et al. (DLCZ) [1] showed that atomic ensembles could be used as nodes of a quantum repeater network capable of sharing pairwise quantum entanglement between systems separated by arbitrarily large distances. In recent years, a number of promising experiments have demonstrated key aspects of this proposal [2, 3, 4, 5, 6, 7]. Here, we describe a scheme for full scale quantum computing with atomic ensembles. Our scheme uses similar methods to those already demonstrated experimentally, and yet has information processing capabilities far beyond those of a quantum repeater.

Amongst the more promising schemes for the implementation of scalable quantum computing are those in which qubits are stored in individual trapped atoms and entangled via single photon interference of photons emitted by the atoms [8, 9]. An appealing aspect of such schemes is that once high-fidelity elementary one- and two-qubit operations can be demonstrated, it is in principle straightforward to scale to a large number of qubits. Notwithstanding recent experimental progress [10], this approach remains experimentally challenging due to the difficulty of trapping and manipulating single atoms, and the difficulty of coupling a single atom to a single optical cavity mode to improve photon collection efficiency.

Atomic ensembles provide a promising alternative system. The atomic excitations of a cloud of  $N$  identical atoms are strongly coupled to the optical field through *collective enhancement* [1], which increases the effective atom-photon coupling by a factor of  $\sqrt{N}$  over the single atom case, negating the requirement for a cavity. Furthermore, it is not necessary for the atoms to be in the Lamb-Dicke limit [11], significantly reducing the trapping and cooling requirements.

We encode a logical qubit in the collective excitations as  $|0\rangle_L \equiv |H\rangle = H^\dagger|G\rangle$  and  $|1\rangle_L \equiv |V\rangle = V^\dagger|G\rangle$ . Here  $S^\dagger = N^{-\frac{1}{2}} \sum S_{(i)}^\dagger$  (for  $S^\dagger = H^\dagger$  or  $V^\dagger$ ) represent symmetric collective excitations of the ensemble, where  $H_{(i)}^\dagger = |H_{(i)}\rangle\langle G_{(i)}|$  denote the excitation operator for atoms, and  $|G\rangle = |G_{(1)}G_{(2)}\dots G_{(N)}\rangle$  is the state with all atoms in the ground state. Two alternative encodings are possible: an internal-state encoding, where the qubit is encoded in two internal atomic levels, in which case  $H_{(i)}/V_{(i)}$  refer to the two metastable energy levels in Fig. 1a; alternatively, a dual rail encoding, where the qubit is encoded in a pair of identical ensembles, each

consisting of atoms with the simpler level structure of Fig. 1b, in which case  $H/V$  label the relevant ensemble. Note that the two ensembles in Fig. 1b may simply be two spatially distinct regions within the same atomic vapour cell, addressed by independent lasers.

A collective excitation, together with a forward-scattered Stokes photon (‘excitation’ panels of Fig. 1), can be generated by weakly driving one arm of the corresponding Raman transition, yielding the state

$$|\psi\rangle = |G\rangle|\text{vac}\rangle + \sqrt{p}S^\dagger s^\dagger|G\rangle|\text{vac}\rangle + O(p), \quad (1)$$

where  $|\text{vac}\rangle$  denotes the vacuum state of the optical mode,  $s^\dagger$  the corresponding photon creation operation operator (which could be  $s^\dagger = h^\dagger$  or  $v^\dagger$ ), and  $p \ll 1$  is the probability of exciting the ensemble. The third term, corresponding to multiple excitations, can be made arbitrarily small relative to the second term by reducing the excitation probability  $p$ . The collective excitation may be measured destructively during ‘readout’, shown in Fig. 1, by driving the reverse transition, resulting in the conversion of the atomic excitations into anti-Stokes photons; the efficiency of this process can be close to unity owing to collective enhancement [7, 11].

Since the qubits are each encoded in separate ensembles (or ensemble pairs) there is no direct interaction between the qubits. Our proposal thus follows DLCZ [1] and entangles separated ensembles using linear optics networks and photodetection on the coherently scattered light. Such entangling operations are non-deterministic, with success heralded by a particular sequence of photodetector clicks. To overcome this indeterminism, we use a form of measurement based QC [12], in which heralded entangling operations can be used to efficiently construct an entangled *cluster state* of many qubits [8, 13, 14, 15]. Such states are described by a graph comprising a collection of edges between qubits. The cluster state corresponding to this graph is defined as the state that results from initializing each qubit in the state  $|+\rangle = (|0\rangle + |1\rangle)/\sqrt{2}$ , and then applying controlled-phase operations  $CZ_{ij} = \text{diag}(1, 1, 1, -1)$  to all qubit-pairs  $i$  and  $j$

\*seandbarrett@gmail.com

†peter.rohde@materials.ox.ac.uk

‡stace@physics.uq.edu.au

linked by graph edges. Once the cluster state has been prepared, universal QC can be implemented by a sequence of single qubit measurements on the state of the form  $\sin(\theta_i)X_i + \cos(\theta_i)Y_i$ . Here  $X_i, Y_i, Z_i$  are the Pauli operators on the  $i$ th qubit, and  $\theta_i$  is a parameter that depends on the outcomes of earlier measurements. These measurements are implemented by mapping the ensemble qubit onto a photon ('readout' of Fig. 1), transforming the photon polarization using standard linear optical elements, then measuring the photon in the  $h$ - $v$  basis.

In the remainder of this paper, we describe a procedure for building a cluster state of atomic ensemble qubits using linear optical networks and photodetection. We first outline a process for *fusing* two arbitrary cluster states together via an optical network that implements a heralded controlled-phase operation. We then describe a protocol for constructing primitive 3-qubit cluster states. Cluster fusion plus 3-qubit cluster states is then sufficient to build arbitrary clusters. The protocol is first described for the idealized case of perfect 'readout', perfect collection and detection efficiency, negligible unwanted excitations, and negligible decoherence of the atomic ensemble qubits. We subsequently argue that the scheme is also robust when these idealizations are relaxed.

For clarity of exposition, we assume that arbitrary local unitary mode transformations can be performed on each ensemble (or pair of ensembles) representing a single qubit. In fact, such operations may be difficult to implement in practice; however, as we describe in the supplementary information, all such operations can be deferred until after the atomic excitations have been mapped onto photon states, and thus can be implemented with standard linear optical elements.

We now describe how to apply a controlled-phase (CZ) gate between two qubits, labelled 3 and 4 in Fig. 2a, each attached to an arbitrary cluster, and each attached to singly linked qubits (labeled 1 and 2). This gate is *destructive* since it consumes qubits 1 and 2, and implements a CZ gate between their neighbours. This operation serves to forge new links between clusters, thereby building larger or more connected graphs.

The (unnormalized) state in Fig. 2a may be written

$$|\Phi\rangle = (H_1^\dagger + V_1^\dagger Z_3)(H_2^\dagger + V_2^\dagger Z_4)|\Phi'\rangle|G\rangle_1|G\rangle_2. \quad (2)$$

The collective excitations in ensembles 1 and 2 are converted to photons using the readout pulse of Fig. 1. The optical output of 1 passes through a Hadamard gate,  $H$ , then is mixed with the output of 2 in the optical circuit shown in Fig. 2b. Immediately before the photons arrive at the photodetectors, the state of the system is given by

$$\begin{aligned} |\Psi\rangle = & [(h_a^\dagger v_a^\dagger - h_b^\dagger v_b^\dagger)Z_4 CZ_{34} \\ & - (h_b^\dagger v_a^\dagger - h_a^\dagger v_b^\dagger)Z_3 Z_4 CZ_{34} \\ & + ((h_a^\dagger)^2 - h_b^\dagger{}^2)(1 + Z_3) \\ & + (v_a^\dagger{}^2 - v_b^\dagger{}^2)Z_4(1 - Z_3)]|\Phi'\rangle|\text{vac}\rangle_{ab}, \end{aligned} \quad (3)$$

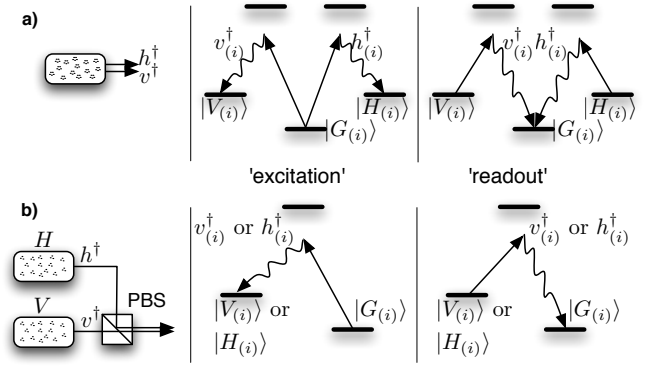


FIG. 1: Configuration and atomic level structure for (a) internal-state encoding: a qubit is encoded in the two internal atomic states  $|H(i)\rangle$  and  $|V(i)\rangle$ , of atoms in a single ensemble and (b) dual-rail encoding: a qubit is encoded in the single atomic state of atoms in two separate but identical ensembles, labelled 'H' and 'V'. The ensembles may be two distinct regions within the same vapour cell, addressed by spatially separated lasers. When operated in 'excitation' mode, a weak, off resonant laser field drives the upward transition (straight lines), and a Stokes photon is emitted (wiggly lines). In 'readout' mode, the frequencies are reversed, producing an anti-Stokes photon in the output mode.

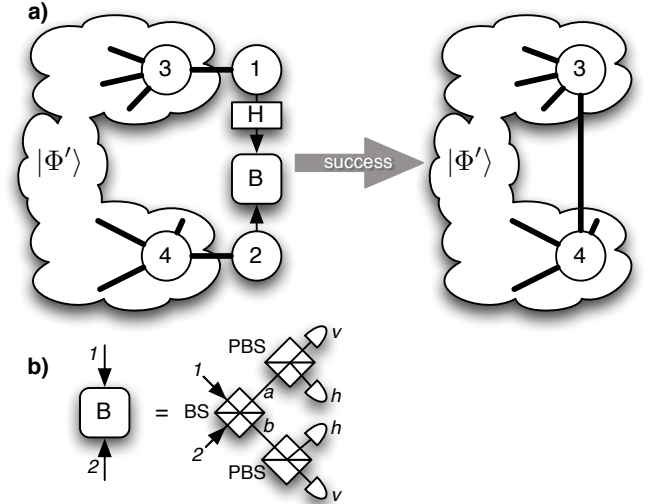


FIG. 2: a) Protocol for implementing a destructive CZ gate between nodes of a cluster state, each designed to have a singly-linked node (nodes 1 and 2), with which to build the link. Readout pulses are applied to ensembles 1 and 2, converting the atomic excitations into photons. The box labelled H is a Hadamard gate on the qubit originally encoded in ensemble 1, which can be implemented via linear optical elements. Note that  $|\Phi'\rangle$  may be a product of two disconnected cluster states, so this operation fuses the two together. b) Box B consists of a beam splitter (BS) and two polarisation sensitive photodetectors. A successful CZ operation is implemented between qubits 3 and 4 when the detected photons are found to have opposite polarisations.

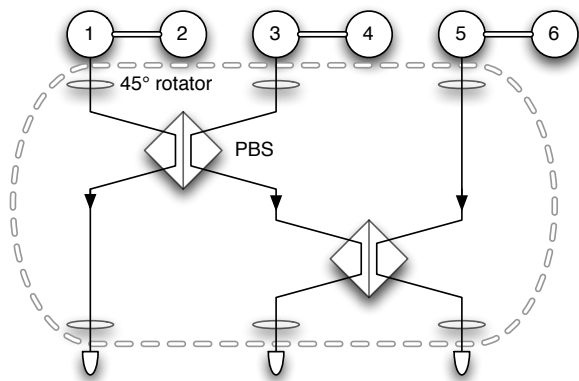


FIG. 3: Protocol for transforming three two-qubit EME states into a three qubit cluster state using polarisation rotators and polarising beam splitters (PBSs). Numbered circles represent atomic ensembles, double lines indicate EME correlations, and thin lines represent optical paths. The dashed line encloses linear optical elements. Readout pulses are applied to qubits 1, 3 and 5. If each of the three detectors register a single photon, ensembles 2, 4 and 6 are projected onto a state that is equivalent, up to local transformations, to a three-qubit cluster state.

where  $a$  and  $b$  label the output modes from the beam splitter. The first two terms in  $|\Psi\rangle$  represent states in which the two photons have different polarisations, and the last term represents states in which the two photons have identical polarisations. Thus when the photodetectors click, with 50% chance the photons are found to have opposite polarisations, and the state is successfully projected onto one that is equivalent (up to local  $Z_i$  operations which must be applied conditional on the outcome) to having a CZ gate applied between ensembles 3 and 4, resulting in a new cluster state with a link between nodes 3 and 4, as shown in Fig. 2a. When photons are registered with the same polarisation, the gate fails, and ensemble 3 is projected onto one of the eigenstates of  $Z_3$ , which has the effect of removing it from the cluster. Thus, in the event of a failure, a total of three ensembles are removed from the initial state.

A cluster state can be efficiently constructed with this non-deterministic but heralded CZ operation: failure of any operation damages the graph, but this can be repaired in subsequent steps. Provided an appropriate strategy is used, the total cost of preparing the state is proportional to the size of the cluster [8, 13, 14, 15, 16, 17, 18, 19].

With our CZ gate, successful fusion of an  $n$  qubit cluster and an  $m$  qubit cluster results in a new cluster of size  $n + m - 2$ . Thus, in order to grow large cluster states, we require an initial supply of 3-qubit cluster states. We now describe a two-step recipe for preparing these states, starting from an initial supply of ensembles in the  $|G\rangle$  state.

The first step is to prepare three copies of an ‘effec-

tive maximally entangled’ (EME) state of two ensembles, which is given by  $|\text{EME}\rangle_{i,j} = (H_i^\dagger + V_j^\dagger)(V_i^\dagger + H_j^\dagger)|G\rangle$  [20]. These states are ‘effectively’ entangled, in the sense that projecting them onto the subspace with a single excitation per ensemble results in a maximally entangled state of two qubits. EME states of two ensembles (or ensemble pairs) may be prepared by first applying a weak  $h^\dagger$  excitation pulse to each ensemble, mixing the forward scattered Stokes photons on a 50/50 beamsplitter, and then detecting the photons with photodetectors. If a single photon is registered, the ensembles are left in one of the states  $(H_i^\dagger \pm H_j^\dagger)|G\rangle$ , depending on which detector clicked. Repeating the procedure with  $v^\dagger$  excitation pulses results in the state  $(H_i^\dagger \pm H_j^\dagger)(V_i^\dagger \pm V_j^\dagger)|G\rangle$ . By applying appropriate local unitary mode transformations, this state can be brought into the form  $|\text{EME}\rangle_{i,j}$ .

While these states may be useful in certain small scale applications [20], the existence of multiple excitation terms are problematic for a scalable quantum computing scheme, since they correspond to *leakage errors* in the computation. We overcome this problem with the network of Fig. 3. This takes as input three EME pairs, and conditional on the correct sequence of measurement outcomes, outputs a *true* three-qubit maximally entangled cluster state, with only a single excitation per qubit. This network was inspired by the observation that a similar network, in an all-optical QC context [21], also removes double excitation terms. Given a supply of ideal EME states, the success rate for this step is  $1/32$  (c.f. [21]).

Our destructive CZ gate together with this initial supply of 3-qubit clusters is sufficient to build arbitrary cluster states with a total cost linear in the size of the clusters. To give an estimate of this cost, our (as yet unoptimized) scheme can produce an  $N$ -ensemble linear cluster state with a total of  $1536N/p$  elementary laser operations (see supplementary information). (Note that  $p$  should be made sufficiently small to reduce the rate of multiple excitation errors in the state).

Physical processes which lead to errors in the computation include atomic decoherence, losses in linear optical elements, imperfect coupling between collective atomic and optical modes [7], and imperfect photo-detection and dark counts [22]. Fault tolerant quantum computation (FTQC) architectures exist for non-deterministic measurement-based schemes [23, 24, 25], so we do not address the general question of how to correct *all* errors in our scheme, but note that FTQC can be implemented, provided the total error rate lies below the FTQC threshold, which is around  $10^{-3} - 10^{-2}$ .

The dominant sources of error in this proposal – imperfect coupling efficiency, photon loss and detector inefficiency – are quantified by the effective readout probability  $\eta$ , that an excitation in a collective atomic mode is firstly mapped by a ‘readout’ pulse into the correct optical mode, then propagates through the optical network and is ultimately detected by a photo-detector. A readout failure thus leads to a *heralded loss* error, signified by the absence of a photo-detection event. In the supplementary

information we draw on previous work [21] to show that heralded loss errors can be tolerated provided  $\eta > 2/3$ , which is much less restrictive than FTQC thresholds for more general error models.

This result is particularly promising for our scheme since many decoherence processes such as thermal motion, atomic dephasing and spontaneous emission simply lower the coupling rate between collective atomic and optical modes [1, 7]. These errors simply reduce  $\eta$  (rather than producing logical errors), so can be tolerated with the very modest threshold for heralded loss errors. This robustness is a consequence of the redundant encoding of the logical qubits in collective modes of many atoms.

We have described a scalable scheme to perform quantum computation with atomic ensembles and linear optics. The scheme uses similar methods to those used in

quantum repeater experiments, and yet our proposal has information processing capabilities far beyond those of a quantum repeater. An important aspect of the scheme is the efficient elimination of doubly-excited components in the created entangled states. A reasonable near future experimental goal is the creation of heralded 3 qubit cluster states (Fig. 3). This involves only a moderate increase in complexity over existing experiments, and would allow interesting applications such as multi-party tests of quantum mechanics [26], and quantum secret sharing [27] in a non-postselected setting.

We thank Ian Walmsley, Virginia Lorenz, Josh Nunn, Simon Benjamin, Gerard Milburn, and Terry Rudolph for useful conversations. SDB is supported by the EPSRC. PPR thanks the QIPIRC (No. GR/S82176/01) for support. TMS is supported by the ARC.

- 
- [1] L.-M. Duan, M. D. Lukin, J. I. Cirac, and P. Zoller, *Nature* **414**, 413 (2001).
  - [2] M. D. Eisaman, L. Childress, A. André, F. Massou, A. S. Zibrov, and M. D. Lukin, *Phys. Rev. Lett.* **93**, 233602 (2004).
  - [3] V. Balić, D. A. Braje, P. Kolchin, G. Y. Yin, and S. E. Harris, *Phys. Rev. Lett.* **94**, 183601 (2005).
  - [4] S.-Y. Lan, S. D. Jenkins, T. Chanelière, D. N. Matsukevich, C. J. Campbell, R. Zhao, T. A. B. Kennedy, and A. Kuzmich, *Phys. Rev. Lett.* **98**, 123602 (2007).
  - [5] Y.-A. Chen, S. Chen, Z.-S. Yuan, B. Zhao, C.-S. Chuu, J. Schmiedmayer, and J.-W. Pan, *Nature Physics* **4**, 103 (2008).
  - [6] K. S. Choi, H. Deng, J. Laurat, and H. J. Kimble, *Nature* **452**, 67 (2008).
  - [7] J. Simon, H. Tanji, J. K. Thompson, and V. Vuletic, *Phys. Rev. Lett.* **98**, 183601 (2007).
  - [8] S. D. Barrett and P. Kok, *Phys. Rev. A* **71**, 060310(R) (2005).
  - [9] Y. L. Lim, A. Beige, and L. C. Kwek, *Phys. Rev. Lett.* **95**, 030505 (2005).
  - [10] D. L. Moehring, P. Maunz, S. Olmschenk, K. C. Younge, D. N. Matsukevich, L. M. Duan, and C. Monroe, *Nature* **449**, 68 (2007).
  - [11] L. Duan, J. Cirac, and P. Zoller, *Phys. Rev. A* **66**, 23818 (2002).
  - [12] R. Raussendorf and H. J. Briegel, *Phys. Rev. Lett.* **86**, 5188 (2001).
  - [13] M. A. Nielsen, *Phys. Rev. Lett.* **93**, 040503 (2004).
  - [14] D. E. Browne and T. Rudolph, *Phys. Rev. Lett.* **95**, 010501 (2005).
  - [15] Y. L. Lim, S. D. Barrett, A. Beige, P. Kok, and L. C. Kwek, *Phys. Rev. A* **73**, 012304 (2005).
  - [16] P. P. Rohde and S. D. Barrett, *New J. of Phys.* **9**, 198 (2007).
  - [17] K. Kieling, D. Gross, and J. Eisert, *J. Opt. Soc. Am. B* p. 184 (2006).
  - [18] D. Gross, K. Kieling, and J. Eisert, *Phys. Rev. A* **74**, 042343 (2006).
  - [19] K. Kieling, T. Rudolph, and J. Eisert, *Phys. Rev. Lett.* **99**, 130501 (2007).
  - [20] L.-M. Duan, *Phys. Rev. Lett.* **88**, 170402 (2002).
  - [21] M. Varnava, D. E. Browne, and T. Rudolph (2007).
  - [22] P. P. Rohde and T. C. Ralph, *J. Mod. Opt.* **53**, 1589 (2006).
  - [23] C. M. Dawson, H. L. Haselgrove, and M. A. Nielsen, *Phys. Rev. Lett.* **96**, 020501 (2005).
  - [24] C. M. Dawson, H. L. Haselgrove, and M. A. Nielsen, *Phys. Rev. A* **73**, 052306 (2006).
  - [25] R. Raussendorf, J. Harrington, and K. Goyal, *Annals of physics* **321**, 2242 (2006).
  - [26] D. Greenberger, M. Horne, A. Shimony, and A. Zeilinger, *American J. of Phys.* **58**, 1131 (1990).
  - [27] M. Hillery, V. Bužek, and A. Berthiaume, *Phys. Rev. A* **59**, 1829 (1999).

## I. SUPPLEMENTARY MATERIAL: OVERCOMING LOSS ERRORS

In this section we consider in more detail the effect of various loss processes within our scheme. In particular, the dominant loss processes are due to photodetector inefficiency (that is, the effect of photodetectors failing to register a ‘click’ when a photon enters a detector) and the effect of imperfect coupling between the atomic ensemble and the correct forward-scattered photon mode. Imperfect ensemble-photon coupling arises from a number of physical processes. Firstly, there is a fundamental limit imposed by the competition between collective coupling of the ensemble to the forward scattered mode, and single-atom spontaneous emission into other free-space modes [1, 7]. Secondly, thermal motion of the atoms can reduce the efficiency of the ensemble-photon conversion process [7]. In addition, a variety of dephasing and relaxation processes which act on the atoms in the ensembles can reduce the effective coupling efficiency [7].

In this work, we model detector inefficiency by replacing each inefficient detector with a perfect one, preceded by a beamsplitter with transmissivity  $\eta_D$ . Similarly, imperfect ensemble-photon coupling processes can be modeled by assuming the ensemble-photon coupling is perfect, but adding a beamsplitter with transmissivity  $\eta_E$  on the output of each ensemble.

An important technique for analysing the effect of these losses is to note that, formally, these beamsplitters can be commuted through other linear optical elements, with the aid of the commutation relations given in [21]. To further simplify the analysis we make the assumption that each detector has the same efficiency  $\eta_D$ , and that the ensemble-photon coupling efficiency takes the same value  $\eta_E$  for every ensemble. We also, for the purposes of this section, ignore all other imperfections such as detector dark counts. This assumption is justified since with modern APD detectors, dark count rates are typically rather low ( $\sim 50 \text{ s}^{-1}$ ).

In the remainder of this section, we consider the effect of these losses at each stage of our protocol, starting at the lowest level (creating two-ensemble EME states), and then considering the higher level processes of creating 3-qubit GHZ states, and bonding clusters with the destructive CZ gate. Our aim is to show that, to a good approximation, these errors can lead to an ‘independently degraded’ (ID) error model, where we can form states that correspond to initially ideal cluster states which have subsequently been subject to uncorrelated qubit loss errors acting independently on each qubit. The effect of such loss errors is to place the affected ensemble qubit in the  $|G\rangle$  state, regardless of its initial state. These ID states can then be used to perform FTQC with a very high threshold [21], corresponding to a loss probability of 0.5 per qubit. Throughout this section, we make substantial use of methods and results due to Varnava et al. [21], who discussed the issue of loss tolerance in the context of all-optical quantum computing.

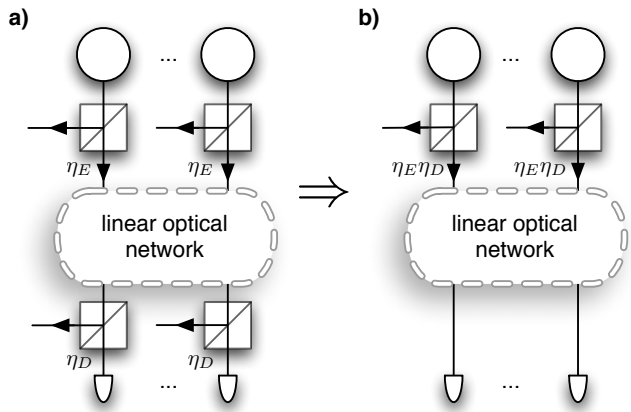


FIG. 4: Commuting detector loss through the beamsplitter in the EME preparation circuit so as to map it to source loss. Now the loss in the system can be characterized in terms of a single efficiency parameter  $\eta = \eta_E \eta_D$  acting on the source.

### A. Effect of losses in EME state preparation

Here we consider the effect of loss at the lowest level of the protocol, i.e. when we try and make EME states of two ensemble qubits. As noted above, there will be two types of loss error at this stage of the protocol, characterized by the detection and coupling efficiencies,  $\eta_D$  and  $\eta_E$ , which we can model by beamsplitters with the corresponding transmissivities (see Fig. 4a). The first step in the analysis is to commute the beamsplitters  $\eta_D$  to the output of each ensemble, leading to an effective model in which the detectors are perfect, but each ensemble has a beamsplitter of effective transmissivity  $\eta = \eta_D \eta_E$  placed at its output (Fig. 4b).

Consider a single ensemble, together with the  $\eta$ -beamsplitter at its output. Immediately after an excitation pulse (acting on, for example, the  $h$  Raman transition of the ensemble), the combined state of the ensemble and the optical fields is [1]

$$\begin{aligned}
 |\psi\rangle_i &= \sum_n \frac{p^{\frac{n}{2}}}{n!} \left( H_i^\dagger h_i^\dagger \right)^n |G\rangle_i |0\rangle_i, \\
 &\rightarrow \sum_n \frac{p^{\frac{n}{2}}}{n!} \left( H_i^\dagger \right)^n \left( \sqrt{\eta} h_i^\dagger + \sqrt{1-\eta} h_l^\dagger \right)^n |G\rangle_i |0\rangle_i |0\rangle_l,
 \end{aligned} \tag{4}$$

where we have performed the beamsplitter transformation  $h_i^\dagger \rightarrow \sqrt{\eta} h_i^\dagger + \sqrt{1-\eta} h_l^\dagger$  on the second line, with  $h_l$  denoting the mode reflected from the beamsplitter (i.e. the lost light).

Ultimately, the protocol for creating the EME states requires post selection of the case where only one detector click is observed (for each round of the protocol) and so the relevant terms in the above expression are those with only a single photon in the  $i$  mode. However, by expanding out Eq. (5) it is clear that, in the presence of loss,

there will be many such terms, each corresponding to a different total number of ensemble excitations,  $\left(H_i^\dagger\right)^n$ . Thus, in the final post selected state, we expect to see additional terms which correspond to *excess* excitations in the two ensembles. This can be shown explicitly by considering the full network for the EME preparation protocol, together with the  $\eta$ -beamsplitters, tracing out the lost modes (i.e. those reflected from the  $\eta$ -beamsplitters) and projecting onto the case where only two detector clicks are observed. The result is a state of the form

$$\rho_{EME,i,j} = (\mathcal{E}_{H_i} \circ \mathcal{E}_{V_i} \circ \mathcal{E}_{H_j} \circ \mathcal{E}_{V_j}) (|EME\rangle_{i,j} \langle EME|), \quad (6)$$

where the excitation superoperators  $\mathcal{E}_S$  are given, up to an overall normalization factor, by

$$\mathcal{E}_S(\rho) = \sum_{i \geq 0} \frac{p^i (1-\eta)^i}{i!} (S^\dagger)^i \rho (S)^i, \quad (7)$$

with  $S^\dagger$  the excitation operator for the corresponding ensemble mode.

These excitation errors take the ensembles out of the logical qubit basis and therefore will lead to errors in the computation. Furthermore, it is not obvious that they can be detected with certainty in subsequent ‘readout’ stages of the protocol, since by assumption the readout and detection efficiencies are less than unity. However, by inspecting Eqs. (6) and (7) it is clear that the probabilities of the error terms are order  $p(1-\eta)$  or higher. Thus the relative contribution of these terms can, in principle, be made arbitrarily small simply by reducing the strength of the excitation laser pulse (which controls the parameter  $p$ ). This comes at the expense of decreasing the success probability for preparing EME states, which incurs a linear increase in the time required to prepare these states. Since EME preparation occurs at the lowest level of the protocol, and since (given sufficient physical resources) many EME states can be prepared in parallel, these errors can be strongly suppressed without affecting the overall efficiency of the computation. For the remainder of this section we therefore treat the EME states as being essentially perfect. In reality, of course, there will be some residual multiple excitation errors, but provided the magnitude of these is sufficiently small they can be dealt with within a more general fault tolerance framework.

## B. Effect of loss in GHZ state preparation

We now consider the effect of losses in the GHZ preparation step. The inputs to this network are three two-qubit EME states, which we assume to be perfect EME states,  $|EME\rangle_{i,j} = (H_i^\dagger + V_j^\dagger)(V_i^\dagger + H_j^\dagger)|G\rangle$ . Our aim here is to demonstrate that, conditional on observing three detector clicks in each of the (polarisation resolving) detectors shown in Fig. 3, the remaining three ensembles

are projected into an ID-loss state. We make use of similarities between our network for converting EME states into GHZ states, and the circuit presented by Varnava et al. [21] for generating GHZ states of photonic qubits.

As in the previous section, we model the photodetector and ensemble-photon coupling efficiencies,  $\eta_D$  and  $\eta_E$ , by beamsplitters with the corresponding transmissivities placed at the inputs to the detectors and outputs to the ensembles, as shown in Fig. 4a (using the linear optical network enclosed by the dashed line in Fig. 3). The first step of the analysis is to make use of the commutation relations for identical beamsplitters to move the  $\eta_E$  beamsplitters forwards through the polarization rotators, and the  $\eta_D$  beamsplitters backwards through the network, to arrive at the equivalent network in Fig. 4b, where the losses are now represented by the three beamsplitters of effective transmissivity  $\eta = \eta_E \eta_D$ .

Varnava et al. showed, via a detailed analysis, that the all-optical circuit of Fig. 5a, with imperfect single photon sources of efficiency  $\eta_S$  (which is unity for a perfect source), leads to a state that is locally equivalent to a 3-qubit ID-GHZ state on the qubits in modes 2, 3 and 5. This state is obtained conditional on a single click being observed at each of the detectors. Assuming that the detectors are perfect, Varnava et al. showed that the output state is an ID-GHZ state with local loss rate  $f = 1 - \frac{\eta_S}{2-\eta_S}$  acting on each qubit.

To make use of this result, first note that the circuit considered by Varnava et al. is equivalent to the one shown in Fig. 5b, in which the beamsplitters representing source inefficiency are commuted through the first row of linear optical elements. Now, if we consider the state of the six photons at the position of the broken line in Fig. 5b, it is found that they have the same form as the three two-qubit EME states at the input to our GHZ network, up to an unimportant polarization rotation acting independently on each mode. Furthermore, the remainder of the optical network lying below the broken line in Fig. 5b is identical to the optical network used in our GHZ network, Fig. 3. Thus we can directly apply the result of [21], which implies that, conditional on a single click being observed in each detector in our network, the final state of ensembles 2, 4, and 6 is the ID-GHZ state

$$\rho_{GHZ,2,4,6} = (\mathcal{L}_{H_2} \circ \mathcal{L}_{V_2} \circ \mathcal{L}_{H_4} \circ \mathcal{L}_{V_4} \circ \mathcal{L}_{H_6} \circ \mathcal{L}_{V_6}) \dots (|GHZ\rangle_{2,4,6} \langle GHZ|). \quad (8)$$

where the loss superoperators  $\mathcal{L}_S$  are

$$\mathcal{L}_S(\rho) = (1-r)\rho + r(S\rho S^\dagger + S S^\dagger \rho S S^\dagger). \quad (9)$$

The loss rate is given by  $r = 1 - (2 - \eta_E \eta_D)^{-1}$ . Note this is slightly different from the value  $f$  determined by Varnava et al., owing to the fact that we have not (as yet) included the effect of coupling and detector efficiencies for the (as yet) unmeasured ensembles 2, 4 and 6.

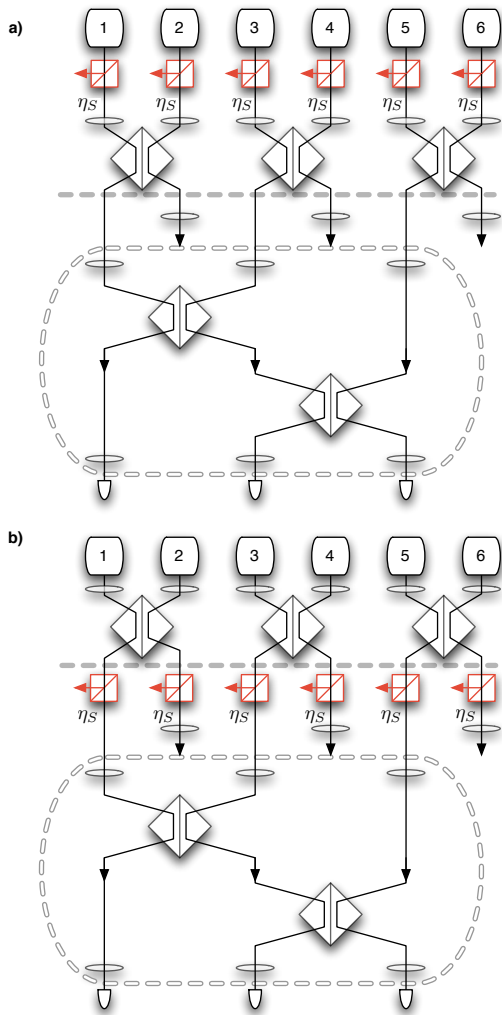


FIG. 5: The equivalence of independent losses (a) before and (b) after the first row of PBS's in the GHZ preparation circuit of Varnava *et al.* Single photon sources 1 to 6 emit an  $H$ -polarised photon. Immediately after the first row of PBSs in (b) (at the dark dashed line) the photons are in the state  $|EME\rangle_{1,2}|EME\rangle_{3,4}|EME\rangle_{5,6}$ .

### C. Effect of loss in cluster state preparation and measurement based computation

To complete the demonstration of loss tolerance in our scheme, we now consider the effect of loss when building large cluster states with our destructive CZ gate, and in the single qubit measurement phase of the computation.

First consider the effect of loss when attempting to fuse two ID-cluster states via our destructive CZ gate, as shown in Fig. 2. As with the other gates, it is possible to model the coupling and detector efficiencies with beamsplitters, and again the  $\eta_D$  beamsplitters can be commuted back through the optical network such that both losses can be represented by a single beamsplitter with transmissivity  $\eta = \eta_E \eta_D$ , at the output of each en-

semble. The CZ gate is non-deterministic, with success heralded by the observation of two detector clicks in separate detectors. Thus, provided the two input states are ID-cluster states, the principal effect of the losses is to reduce the overall success rate of the gate by a factor  $\eta/(2 - \eta)$ . Note that this rate is a product of the loss rate,  $r$ , of the input ID-cluster states, together with the additional losses incurred in the CZ gate itself. Upon success, the resulting larger cluster state will be an ID state with the same loss rate as the input states. This means that the CZ gate can be used to build up large ID-cluster states of arbitrary shape, and, assuming that additional losses incurred while these cluster states are being constructed are negligible, the effective loss rate for these clusters will be  $r = 1 - (2 - \eta)^{-1}$ .

The other effect of loss in the CZ gate is that new 'failure outcomes' of the gate should now be considered. As well as the original failure outcome - observing two photons in the same mode - we must also consider the case when only one or zero clicks are observed. In this case, the input state  $|\Phi'\rangle$  in Fig. 2 is left in an indeterminate (i.e. mixed) state. However, it is generally possible to recycle significant parts of the input clusters by performing a successful  $Z$  measurement on qubits '3' and '4'.

The final stage of our scheme where we must consider the effect of loss is the 'readout' phase of the measurement based computation. In this phase, each qubit in the constructed cluster undergoes a single qubit measurement, which comprises a 'readout' pulse on the ensemble(s), followed by some linear optical operations on the output photons, and finally photodetection of the resulting photon state. Clearly, losses will be important here since failure to register a photon in one of these measurements will render the remaining part of the cluster in an indeterminate state. Again, we can make use of the results of Varnava *et al.* [21], who gave an explicit protocol for dealing with this loss model. This involves encoding each logical qubit in a 'tree structure' comprising several physical qubits. Provided the total effective loss rate for the computation (i.e. the combination of the underlying loss rate of the initial cluster, combined with the additional losses in the single qubit readout phase) is less than  $1/2$ , efficient quantum computation is possible. This leads to the final result: losses due to imperfect ensemble-photon coupling and detector efficiencies can be tolerated provided

$$\frac{\eta}{2 - \eta} > \frac{1}{2}, \quad (10)$$

i.e. provided  $\eta > 2/3$ .

## II. SUPPLEMENTARY MATERIAL: RESOURCE USAGE

In order to give an estimate of the resources required by our scheme, we calculate the cost of preparation of linear clusters in terms of the total number of elementary

laser pulses required to build a linear cluster of length  $N$ . Although linear clusters are not sufficient for performing arbitrary computations, they can serve as a resource state for building up larger clusters of arbitrary shape, with moderate additional overhead.

There are several stages of the protocol to consider, which we consider independently. At the lowest level of the protocol we prepare EME states from two separable ensembles. EME preparation consists of two rounds, where each round is independent and heralded. On average this requires  $2/p$  pulses before success.

Now consider the resource consumption of the protocol for making 3-qubit cluster states of Fig. 3. This network takes as an input three 2-qubit EME states. It then successfully bonds these EME's together into a 3-qubit cluster with probability  $1/32$ . Thus the number of operations (i.e. laser excitation pulses) per 3-qubit cluster state is  $3 \times 32 \times 2/p = 192/p$ .

Next, suppose our procedure for building up large linear clusters is as follows: we have a 'main' cluster, which we are attempting to grow, and smaller ancillary clusters which we attempt to bond onto the main cluster. Because our destructive CZ gate succeeds with probability 50%, it can be seen that the ancillary clusters must be of size at least four qubits if the main clusters is to grow on average following each bonding attempt. Thus, we now turn our attention to building 4-qubit ancillary clusters.

Preparing a 4-qubit linear cluster requires two 3-qubit linear clusters. Given two such states they can be successfully bonded together to form a 4-cluster with probability 50%. Thus, the total number of operations per 4-cluster is  $2 \times 2 \times 192/p = 768/p$ .

Given a resource of ancillary 4-clusters, the 'main' cluster can be grown at an average rate of  $1/2$  qubit per bonding attempt. So the total number of operations per final qubit in the cluster is  $2 \times N \times 768/p = 1536N/p$ . Note that, given sufficient experimental resources, many of the above steps can be performed in parallel and so the actual number of time steps required to grow cluster states can be much less than the total number of elementary laser operations.

Here we have adopted an 'incremental' approach to building up long clusters, and at several stages we have assumed that upon a gate failure, the remaining fragments of the ancillary clusters are not recycled. Note that several alternate strategies could be employed when preparing large clusters [16, 17, 18, 19], which might be significantly more resource efficient than the incremental approach considered here.

### III. SUPPLEMENTARY MATERIAL: SINGLE QUBIT OPERATIONS

Throughout the description of the scheme in the main section of the paper, we assumed that local unitary mode

transformations can be performed on each ensemble, or, in the case of the dual rail encoding, on each pair of ensembles corresponding to a single qubit. Such operations may be difficult to implement in practice, particularly in the case of dual rail encoding. Here we describe how these operations can in fact be deferred until the atomic excitations are mapped onto photonic states.

Such single qubit operations are necessary at several stages of the protocol: (1) during the production of the EME states; (2) during the production of the three-qubit cluster states; (3) after CZ operations between nodes of a cluster state; (4) during the 'readout' phase of the measurement based computation, when each qubit is subject to a measurement of the observable  $\sin(\theta_i)X_i + \cos(\theta_i)Y_i$ .

A generic state of  $n$  atomic ensembles may be written

$$|\psi\rangle = f(H_1^\dagger, V_1^\dagger, \dots, H_i^\dagger, V_i^\dagger, \dots, H_n^\dagger, V_n^\dagger) |G\rangle^{\otimes n}$$

where  $f(\dots)$  is a function of the excitation operators acting on each ensemble. A local unitary mode transformation on the modes of the atomic ensemble,  $U_i^{(a)}$ , transforms this state as

$$U_i^{(a)} |\psi\rangle = f(H_1^\dagger, V_1^\dagger, \dots, H'_i{}^\dagger, V'_i{}^\dagger, \dots, H_n^\dagger, V_n^\dagger) |G\rangle^{\otimes n}$$

where

$$\begin{pmatrix} H'_i{}^\dagger \\ V'_i{}^\dagger \end{pmatrix} = \mathbf{U}_i \begin{pmatrix} H_i^\dagger \\ V_i^\dagger \end{pmatrix}$$

with  $\mathbf{U}_i$  a  $2 \times 2$  unitary matrix. Subsequently, applying the readout operation  $R_i$  to the ensembles representing the  $i$ 'th qubit transforms  $H_i^\dagger \rightarrow h_i^\dagger$  and  $V_i^\dagger \rightarrow v_i^\dagger$ :

$$R_i U_i^{(a)} |\psi\rangle |vac\rangle_i = f(H_1^\dagger, V_1^\dagger, \dots, h'_i{}^\dagger, v'_i{}^\dagger, \dots) |G\rangle^{\otimes n} |vac\rangle_i$$

with the photon operators given by

$$\begin{pmatrix} h'_i{}^\dagger \\ v'_i{}^\dagger \end{pmatrix} = \mathbf{U}_i \begin{pmatrix} h_i^\dagger \\ v_i^\dagger \end{pmatrix}.$$

Inspecting the above expressions, it is clear that  $R_i U_i^{(a)} |\psi\rangle |vac\rangle_i = U_i^{(o)} R_i |\psi\rangle |vac\rangle_i$ , where  $U_i^{(o)}$  is a unitary mode transformation on the  $i$ th optical mode with the same unitary mode transformation matrix  $\mathbf{U}_i$  as  $U_i^{(a)}$ . In other words, local unitary mode transformations of atomic ensemble modes can be deferred until after the readout pulse, and performed on the optical modes instead. Such transformations are straightforward to implement with linear optical elements. The particular sequence of such operations that must be performed generally depends on the outcomes of earlier measurements in the scheme, and so a modest amount of classical processing and optical switching is also required.